Nat. Hazards Earth Syst. Sci. Discuss., 2, 3015–3063, 2014
www.nat-hazards-earth-syst-sci-discuss.net/2/3015/2014/
doi:10.5194/nhessd-2-3015-2014

Natural Hazards and Earth System Sciences
Open Access
Discussions

Seismic vulnerability and risk assessment of Kolkata City, India

S. K. Nath, M. D. Adhikari, N. Devaraj, and S. K. Maiti

Department of Geology & Geophysics, Indian Institute of Technology Kharagpur, 721302, West Bengal, India

Received: 10 December 2013 – Accepted: 17 March 2014 – Published: 30 April 2014

Correspondence to: S. K. Nath (nath@gg.iitkgp.ernet.in)

Published by Copernicus Publications on behalf of the European Geosciences Union.

Abstract

The city of Kolkata is one of the most urbanized and densely populated regions in the world, which is a major industrial and commercial hub of the Eastern and North-eastern region of India. In order to classify the seismic risk zones of Kolkata we used seismic hazard exposures on the vulnerability components namely, landuse/landcover, population density, building typology, age and height. We microzoned seismic hazard of the City by integrating seismological, geological and geotechnical themes in GIS which in turn is integrated with the vulnerability components in a logic-tree framework to estimate both the socio-economic and structural risk of the City. In both the risk maps, three broad zones have been demarcated as "severe", "high" and "moderate". There had also been a risk-free zone in the City. The damage distribution in the City due to the 1934 Bihar-Nepal Earthquake of M_w 8.1 well matches with the risk regime. The design horizontal seismic coefficients for the City have been worked out for all the predominant periods which indicate suitability of "A", "B" and "C" type of structures. The cumulative damage probabilities in terms of "slight", "moderate", "extensive" and "complete" have also been assessed for the significant four model building types viz. RM2L, RM2M, URML and URMM for each structural seismic risk zone in the City. Both the Seismic Hazard and Risk maps are expected to play vital roles in the earthquake inflicted disaster mitigation and management of the city of Kolkata.

1 Introduction

The necessity of evaluation of seismic risk of existing built-up regions in terms of damage potential of its urban structures and socio-economic set-up when impacted by a deadly earthquake has become an important issue in the Indian context after the occurrence of Killary (1993) of M_w 6.2, Jabalpur (1997) of M_w 5.8, Chamoli (1999) of M_w 6.8, Bhuj (2001) of M_w 7.7, Kashmir (2005) of M_w 7.6 and Sikkim (2011) of M_w 6.9 earthquakes causing widespread damage and extensive loss of life and property.

The number of fatalities in an earthquake is associated with the vulnerability of local buildings, population density and the intensity of ground shaking. Vulnerability Exposure refers to all man-made facilities namely, the residential, commercial, and industrial buildings, schools, hospitals, roads and railroads, bridges, pipelines, power plants, communication systems, and so on. For the safety and sustainability of urban regions, it is necessary to implement long-range urban planning and risk assessment tools that rely on an accurate and multidisciplinary urban modeling. The Kolkata metropolitan city is among the most densely populated regions in the world and being a major business and industrial hub supports vital industrial and transportation infrastructures. The metropolitan city being placed on the border of Seismic Zones III and IV as per the seismic zoning map of India (BIS, 2002) with a sedimentary thickness of the order of 7.5 km above the crystalline basement is highly vulnerable to earthquake disasters.

2 The city of Kolkata

The Kolkata metropolis, the second largest urban agglomeration in India bounded by latitudes 22°27′–22°40′ N and longitudes 88°18′–88°28′ E has developed primarily along the eastern bank of the River Hooghly about 150 km north of the Bay of Bengal, right over the Ganges delta. The population of Kolkata was 1.5 million in the year 1901 that increased to 11 million in 1991 and a phenomenal increase to 14 million as per the Census report of 2011, due to enormous population pressure it has encroached into the back swamp and marshy land to the east filling up extensive areas, especially in the Salt Lake and Rajarhat regions and many more in an unplanned manner. More than 80 % of the city has built up areas with high rise residential buildings, congested business districts, hospitals and schools etc. some of which are very old with unplanned structures adhering to non-seismic safety standards. Demography in some parts of the city exhibit population density above 100 000 per square kilometer. Figure 1 depicts the study region alongwith some typical urban attributions of the City.

Kolkata is situated in the Bengal Basin, a huge pericratonic Tertiary basin with enormous thickness of fluvio-marine sediments (Dasgupta et al., 2000). The Bengal basin can be divided into three structural units; the westernmost shelf or platform, the central hinge or shelf/slope break and deep basinal part in the east and southeast that presently open in the Bay of Bengal. Kolkata is located over the western part of the hinge zone across which sediment thickness and facies significantly varies from shelf area in the west to the deep basinal part in the east. The most prominent tectonic feature in the Bengal basin is the NE–SW trending Eocene Hinge Zone (EHZ), also known as Calcutta–Mymensing Hinge Zone. The EHZ is 25 km wide extending to a depth of about 4.5 km below Kolkata. The Hinge zone and the deep basin are overlain by thick alluvium to a maximum depth of about 7.5 km. The tectonic grains of Main Boundary Thrust (MBT), Main Central Thrust (MCT), Main Frontal Thrust (MFT), Dhubri Fault, Dauki Fault, Oldham Fault, Garhmoyna–Khandaghosh Fault, Jangipur–Gaibandha Fault, Pingla Fault, Debagram–Bogra Fault, Rajmahal Fault, Malda–Kishanganj Fault, Sainthia–Bahmani Fault, Purulia Shear Zone, Tista Lineament, and Purulia lineament largely influence the seismicity of the region. Besides its nearby sources Kolkata is affected by the far away sources like Bihar-Nepal seismic zone, Assam Seismic Gap, Shillong Plateau, Andaman–Nicobar seismic province, and the N–E Himalayan extent.

The City has been rocked time and again by both near and far field earthquakes of moderate to large magnitudes. Among the far source earthquakes that was felt in Kolkata include the events of 1897 Shillong Earthquake of M_w 8.1, 1918 Srimangal earthquake of M_w 7.6, 1930 Dhubri earthquake of M_w 7.1, 1934 Bihar-Nepal earthquake of M_w 8.1, 1950 Assam Earthquake of M_w 8.7 and 2011 Sikkim Earthquake of M_w 6.9. The Bihar-Nepal earthquake of M_w 8.1 induced MMI intensity of the order of VI–VII in Kolkata and caused considerable damage to life and property (GSI, 1939). The two near source earthquakes reported in Kolkata are the 1906 Kolkata Earthquake with intensity V–VI (Middlemiss, 1908) and the 1964 Sagar Island earthquake of M_w 5.4 with damage intensity of VI–VII surrounding the City (Nath et al., 2010). However, the maximum intensity reported in Kolkata is MMI VII generated from both the near source

NHESSD
2, 3015–3063, 2014

earthquake of 1964 and the distant earthquakes of 1897 and 1934 making the City highly vulnerable to seismic threat (Dasgupta et al., 2000).

3 Vulnerability exposures and thematic data layer preparation

Unplanned urbanization defying building codes are continuously increasing the earthquake vulnerability of Kolkata necessitating the assessment of earthquake vulnerability by identifying those factors contributing to seismic risk in terms of socio-economic and structural aspects. To understand the vulnerability of the built environment and infrastructure, a spatial/non-spatial database of building typology, building height, building age, landuse/landcover, population density and lifeline utilities has been created. These elements at earthquake risk have been studied for different vulnerability level in the seismic hazard microzonation. Vulnerability Index (VI) of different factors is calculated by defining an ordinal scale and overall vulnerability index maps of the study area have been prepared representing socio-economic and structural vulnerability. Figure 2 depicts a framework for seismic Vulnerability and Risk Assessment protocol for the City of Kolkata.

The most common way to represent the confidence level in the assessment of remote sensing data is in the form of computing an error matrix (Congalton, 1991). We derive error matrices for both the structural and socio-economic vulnerability exposures for comparisons. It is based on the widely used accuracy assessment technique of statistical correlations between two map data – one categorized from the Rapid Visual Screening (RVS) which we term as “reference” and the other derived exclusively from remote sensing data which is termed as “classified” (Story and Congalton, 1986; Jensen, 1996). The correlation indicators used in the present analysis include “overall accuracy” i.e. the percentage of matched data between the “reference” and the “classified” maps, “user’s accuracy” i.e. the percentage of matched data in the “classified” map, “producer’s accuracy” i.e. the percentage of matched data in the “reference” map, and the kappa value defining a measure of the differences between the “reference” and

NHESSD
2, 3015–3063, 2014

the chance agreement between both the maps. The kappa value can be expressed as,

$$k = \frac{N \sum_{i=1}^{r} X_{ii} - \sum_{i=1}^{r} (X_{i+} X_{+i})}{N^2 - \sum_{i=1}^{r} (X_{i+} X_{+i})} \quad (1)$$

Where, N is the total number of sites in the matrix, r is the number of rows in the matrix, X_{ii} is the number in row i and column i, $\boldsymbol{X}_{i+}$ is the total for row i, and $\boldsymbol{X}_{+i}$ is the total for column i (Jensen, 1996; Congalton and Mead, 1983). The kappa statistics > 0.80 suggests "strong" agreement, a value within a range of 0.60–0.80 suggests "good" agreement and the chance of agreement is remote while kappa is close to 0 indicating "poor" agreement (Landis and Koch, 1977). The "Margfit" procedure has also been used on each error matrix through the application of a FORTRAN code "Margfit" available in Congalton et al. (1991). The underlying methodology utilizes an iterative proportional fitting to conform to the sum of each row and column in the error matrix to a predetermined value. A normalized accuracy is calculated by summing the values on the major diagonal and dividing it by the sum of the total values in the normalized error matrix (Congalton and Green, 1999). As a result, both the producer's and user's accuracies have been incorporated in the normalized cell value which is based on a balanced effect of these two accuracy measures (Congalton and Green, 1999). In the present study, the structural and socio-economic vulnerability exposures derived from satellite imagery in case of building typology & landuse/landcover and that generated from Google Earth 3-D aspect for building height are used as "classified" data while those derived through Rapid Visual Screening from 1200 survey locations being considered as "reference" data have been used for the accuracy assessment of all the themes. For Rapid Visual Screening a hand held GPS (Global Positioning System) is used for coordinate generation at each of the 1200 locations and the survey

NHESSD
2, 3015–3063, 2014

is conducted on the vulnerability types as has been depicted in Fig. 3 for sample RVS for building heights at four locations in the City.

The key issue for studying the earthquake vulnerability and seismic risk of urban areas is the availability of maps and statistical information that concern the infrastructure of the urban centers (Sarris et al., 2010). For the best possible assessment of the vulnerability and risk of an earthquake prone district, it is necessary to have the maximum possible information such as the one proposed by HAZUS (Sarris et al., 2010) risk assessment model that require detailed inputs on structural configuration in terms of design, shape, height and number of stories, building proximity, lateral strength, stiffness, ductility, foundation, material and its construction practice etc. The focus is on building-specific study from building inventory of group of buildings with similar characteristic and classification. However in the present investigation we proposed an alternative approach based on Satellite Imagery, Google Earth and Rapid Visual Screening for a broader estimation of socio-economic and structural vulnerability of the City of Kolkata and its seismic risk thereof. The seismic hazard is generally assumed to be stable over a long geological time while the typical vulnerability (and, therefore, the risk) to the hazard changes (McGuire, 2004).

3.1 Demography

Population vulnerability exposure can easily be estimated with the help of census data, which will normally give the average number of persons per parcel/ward and also relation to building types. The population of urban Kolkata increased from 1 510 008 in 1901 to 14 112 536 in 2011 as illustrated in Table 1. Total population, population density, and female population, age-wise population below 7 and above 65, day and night time population, illiterate and unemployment population are more vulnerable to seismic shaking. This is well exemplified by the questionnaire for 2011 Indian Census. From Fig. 4 it is observed that the population density is very high in Barabazar, Taltala, Kalidaha, Beniatola, Khidirpur, Metiaburuz and Shyambazar region.

3.2 Landuse/landcover (LULC)

LULC provides information about the predominant urban land cover and socio-economic attributes that can be extracted by carrying out an object-oriented LULC classification on National Atlas and Thematic Mapping Organization (NATMO) nomenclature. LULC classes are mainly defined by the alignment of buildings, streets, agricultural land, vegetation, plantation, water body, open-spaces etc. In the present study LISS-IV and PAN 2010 (NRSC Data Center, ISRO) data have been classified based on maximum likelihood method. LULC map of Kolkata is shown in Fig. 5. The entire study region has been classified into ten major LULC units: residential commercial and industrial area, river/pond/water body, plantation, open space, vegetation/grassland, swampy land, dry fellow land, cultivated land, canal and arable land. The accuracy statistics between the RVS derived "reference" and the LISS IV derived "classified" maps have been presented in Table 2.

3.3 Building typology

The type of materials used in construction is one of the most important attributes in evaluating vulnerability to seismic hazard. Through visual interpretation techniques, using image elements such as tone, texture, shape, size, shadow, pattern, association and location, the building footprint map can be prepared with the help of poor spectral and spatial resolution imageries. LANDSAT TM imagery has been used in this study because of its finer spectral resolution compared to other commonly used images such as SPOT and Multi-Spectral Scanner (MSS). In the present study, we have performed PCA (Principal Component Analysis), Textural Analysis and Normalized Differences Building Index (NDBI) for the identification of building materials (Geneletti and Gortea, 2003; Lu and Weng, 2005; Zhang et al., 2002 and Zha et al., 2003).The building materials have been categorized into 5 classes (A1 – mud and unbrick wall, A2 – stone wall, B – burnt bricks building/buildings of the large block and prefabricated type/building in natural hewn stone, C1-i concrete building and C1-ii newly built-up concrete building) are followed according to BMTPC, (1997) and among them the use of reinforced concrete blocks is dominating the area as depicted in Fig. 6. The Vulnerability Curves for the observed damage (GSI, 1939) due to 1934 Bihar-Nepal earthquake of M_w 8.1 for RCC, steel, masonry and non-engineered structures in Kolkata and adjoining regions have been constructed following Sinha and Adarsh (1999) as presented in Fig. 7. The accuracy statistics between the RVS derived "reference" and the LISS IV & LANDSAT TM derived "classified" maps have been presented in Table 3.

3.4 Building age

Urban population of Kolkata has grown tremendously in the last four decades. This fast rate of increase in urban population is mainly due to large scale migration of people from rural and smaller towns to bigger cities in search of better employment opportunities and good life style. Remote sensing imagery is ideally used to monitor and detect urban land cover changes that occur frequently in urban and peri-urban areas as a consequence of incessant urbanization (Zha et al., 2003). Land covers in urban areas tend to change more drastically over a short period of time than elsewhere because of rapid economic development. In the present study, the built-up areas were obtained from the LANDSAT TM, ETM and MSS classified images of eight different periods (1975, 1980, 1985, 1990, 1995, 2000, 2005 and 2010) to monitor the dynamic changes of urban sprawl (Small, 2002; Zhang et al., 2002). For the purpose, we have used Normalized Difference Built-up Index (NDBI) for classification of built-up areas (Zha et al., 2003). Change detection analyses describe the differences between the images of the same scene at different periods. The building age/urban growth of Kolkata have been estimated using change detection technique in ERDAS IMAGINE 9.0 software as depicted in Fig. 8. For the map validation purposes we have selected a sample block in the New-town financial and infrastructural hub of Kolkata where Landsat TM and Google Earth imageries of 2005 and 2010 have been considered as "classified" and "reference" data sets respectively for urban growth assessment and its allied error statistics. Figure 9 depicts the urban expansion during the period 2005–2010 based on both Landsat TM and Google Earth Imageries. The associated error matrix is given in Table 4. It is seen that the optimal lifetime of structures in Kolkata is between 40–50 yr. The urban expansion has been divided into seven clusters such as, younger than 10 yr, 10–20 yr, 20–30 yr, 30–35 yr, 35–40 yr, 40–50 yr and older than 50 yr as depicted in Fig. 8. The older buildings (> 50 yr) have been adopted from "Atlas of the City of Calcutta and its Environs" (Kundu and Aag, 1996). However, older buildings are likely to be vulnerable to severe damage or total collapse under strong seismic excitations. There are many aged ill-conditioned, closely spaced structures in Kolkata which also seem to be highly vulnerable to seismic threat.

3.5 Site-Structure quasi-resonance and possibility of damage

The response of a building to seismic shaking at its base depends on the design quality of construction. The most important factor is the height of the building. The type of shaking and the frequency of shaking depend on the structure as well as the site of its construction. The fundamental frequency of structures may range from about 2 Hz for a low structure up to about 4 stories, and between 0.5–1 Hz for a tall building from 10–20 stories; thus the tall buildings tend to amplify the longer period motions compared to small buildings (Kramer, 1996). Each structure has a resonance frequency that is the characteristic of the building. Therefore, in developing the design strategy for a building, it is desirable to estimate the fundamental periods both of the building and the site on which it is to be constructed so that a comparison can be made to understand the possibility of quasi-resonance. In the present study, Google Earth and about 1200 ground truth GCP have been used for visual identification of building height using 3-D aspect and its validation. In Fig. 10 the building height map of Kolkata is presented. The accuracy statistics between the RVS derived "reference" and the Google Earth derived "classified" maps have been presented in Table 5. The building heights have been categorized into 5 classes; houses – 1 floor, buildings – 2 to 4 floors, tall buildings – 5 to 8 floors, multistoried buildings – 9 to 10 floors and skyscrapers > 10 floors. Therefore, the approximate fundamental natural period of vibration (T_a), in seconds, has been estimated by the empirical expression (BIS, 2002);

$$\begin{aligned} T_a &= 0.075h^{0.75} \quad \text{for RCC frame building} \\ &= 0.085h^{0.75} \quad \text{for steel frame building} \\ &= \frac{0.09h}{\sqrt{d}} \quad \text{all other buildings} \end{aligned} \tag{2}$$

Where, "T_a" = fundamental period of vibration in seconds "h" = height of the building in meters. d = base dimension of building at plinth level in "meters", along the considered direction of the lateral force.

The site fundamental period has been estimated from microtemor H/V power spectral ratio (Nakamura, 1989) based on the following equation:

$$H/V_{\text{spectral ratio}} = \sqrt{\frac{\sum P_{NS}(\omega) + \sum P_{EW}(\omega)}{\sum P_V(\omega)}} \tag{3}$$

Where, $P_{NS}(\omega)$, $P_{EW}(\omega)$ and $P_V(\omega)$ are the power spectra of NS, EW and the vertical components respectively, summation is taken over the data blocks. The H/V response curves obtained from the microtremor survey reflects the geology and soil properties of the test site. Lermo and Chavez-Garcia (1993) examined the relevance of HVSR for weak and strong motion earthquake records and found good agreement in the soil resonance frequencies. Using 1-D models of shear wave velocity, they validated the applicability of HVSR. Ambient noise data acquired using SYSCOM MR2000 at 1200 locations in the City have been processed using View2002 and GEOPSY software (www.geopsy.org). The Predominant Frequency distribution map shown in Fig. 11 is prepared on GIS platform exhibiting a variation between 0.6 Hz to 3.1 Hz. The proximity of Predominant Frequency of the soil column and the natural frequency of life line facilities indicates higher vulnerability of the built-up environment owing to resonance effects (Nath and Thingbaijam, 2009). Normally, the natural period of vibration of any structure should not coincide with the predominant period of earthquake excitations, otherwise resonance may occur and even the strongest structure may collapse (BIS, 2002). Figure 12 represents the difference between the structure's natural period of vibration and the predominant period of the respective site indicating damage possibilities of existing structures/logistics due to the impact of an earthquake – the larger the difference the lesser is the possibility of destruction.

4 Seismic Hazard Microzonation of Kolkata

Seismic hazard can be estimated by analyzing past earthquakes' activity in the region, evidence of stress-bearing of structures within fault area and how seismic waves travel through the crust alongwith overlying soils beneath the sites (Panahi et. al., 2013). Worthy to be noted that at the time of an earthquake in addition to peak ground acceleration (PGA), the incidence of soil liquefaction and slope failure are the secondary phenomena which can cause increasing seismic vulnerability and damage. Multi-criteria assessment for seismic hazard leading to seismic microzonation is the key factor to understanding the overall seismic risk of a region. The hazard mapping is achieved through multi-criteria based decision support system formulated by Saaty (1980) as Analytical Hierarchal Process (AHP). The hazard themes, pertaining to the study region materialized as thematic layers on the GIS platform are (i) Peak Ground Acceleration (PGA) with 10 % probability of exceedance in 50 years at surface, (ii) Liquefaction Potential Index (LPI), (iii) NEHRP Site Class (SC), (iv) Sediment Class (SEC), (v) Geomorphology (GM), and (vi) Ground Water Table (GWT) as shown in Fig. 13a–f. The details of each theme have been discussed in Nath et al. (2014). In the present study ArcGIS 9.3 has been used for the purpose of thematic mapping through vector layer generation and spatial analysis. Each thematic layer has been geo-rectified on Universal Transverse Mercator (UTM) projection system.

The major geomorphological units present in Kolkata are deltaic plain, interdistributory marsh, paleo-channels, younger levee adjacent to river Hoogly and older levee on both sides of the Adi Ganga (Roy et al., 2012) as depicted in Fig. 13a. Based on the proportions of sand, silt and clay-sized particles obtained from 350 boreholes in Kolkata, the bottom sediments have been classified according to Shepard's diagram (O'Malley, 2007) that exhibit highly liquefiable sediments viz sand, sand-silt clay, sandy clay, silty sand and silty clay upto about ~ 5 m as shown in Fig. 13b. Ground water table depth is among the major contributors affecting the stability of the soil column. The water table depths obtained from 350 boreholes calibrated with post monsoon piezometer survey are used to generate a water table depth variation map of the City as shown in Fig. 13c depicting water table fluctuation between 0.1–7.7 m. Site classification of Kolkata performed using in-depth geophysical and geotechnical investigations from 350 borehole data based on NEHRP, USGS and FEMA nomenclature places the City in D1 (V_s^{30}: 180–240 m s^{-1}), D2 (V_s^{30}: 240–300 m s^{-1}), D3 (V_s^{30}: 300–360 m s^{-1}) and E ($V_s^{30} < 180$ m s^{-1}) classes as shown in Fig. 13d. The Probabilistic Seismic Hazard Assessment at surface consistent level performed by propagating the bedrock ground motion with 10 % probability of exceedance in 50 years through 1-D sediment column using an equivalent linear analysis of an otherwise nonlinear system predicts a Peak Ground Acceleration variation from 0.176 g to 0.253 g in the City as depicted in Fig. 13e. There had been evidences of wide spread liquefaction in Kolkata triggered by the 1934 Bihar-Nepal Earthquake of M_w 8.1. Therefore, soil liquefaction in terms of Factor of Safety against liquefaction is considered as one of the major contributors of seismic hazard potential in Kolkata and is, therefore, used in the present microzonation protocol. The standard methodology given by Youd et al. (2001), Idriss and Boulanger (2006) and Iwasaki et al. (1982) based on SPT-N value is used for liquefaction susceptibility computation considering surface PGA distribution with 10 % probability of exceedance in 50 years. LPI values have been categorized according to Iwasaki et al. (1982) as: non-liquefiable (LPI = 0), Low ($0 < \text{LPI} < 5$), High ($5 < \text{LPI} < 15$) and Severe ($\text{LPI} > 15$) as shown in Fig. 13f.

The corresponding weights and the ranks to each thematic layer and the feature ranks thereof are assigned values accordingly to the apparent contribution of the layers to the overall seismic hazard (Nath, 2004). All the geo-referenced thematic layers

NHESSD
2, 3015–3063, 2014

are integrated step-by-step using the aggregation method in GIS to generate Seismic Hazard Microzonation Map (SHM) as

$$\mathrm{SHM} = [\mathrm{PGA}_w\mathrm{PGA}_r + \mathrm{LPI}_w\mathrm{LPI}_r + \mathrm{SC}_w\mathrm{SC}_r + \mathrm{SED}_w\mathrm{SED}_r + \mathrm{GM}_w\mathrm{GM}_r + \mathrm{GW}_w\mathrm{GW}_r]/\sum w \tag{4}$$

Where, "w" represents the normalized weight of a theme and "r" is the normalized rank of a feature in the theme. Thereafter, a 3×3 "majority filter" has been applied to the SHM as a post-classification filter to reduce the high frequency variation. SHM is a dimensionless quantity that helps in indexing the probability of seismic hazard and hence the microzonation of a region on a qualitative scheme such as "Low", "Moderate", "High" and "Severe". The Probabilistic Seismic Hazard Microzonation map of Kolkata is shown in Fig. 13g. Four broad divisions have been identified with hazard index (HI) defined as, $0.68 < \mathrm{HI} \leq 0.88$ indicating Severe hazard condition in Salt Lake area, $0.47 < \mathrm{HI} \leq 0.68$ indicating High hazard condition mostly in Rajarhat, New Town areas of the expanding City, $0.27 < \mathrm{HI} \leq 0.47$ indicating moderate hazard condition in the most part of South and West Kolkata, while $\mathrm{HI} < 0.27$ represent low hazard condition. The damage distribution due to the Great 1934 Bihar-Nepal Earthquake of M_w 8.1 is reported to have induced an MMI intensity VI-VII in Kolkata (GSI, 1939) mostly identified in the moderate to High Hazard zone (marked by a star (*)).

5 Multicriteria seismic risk assessment

Ishita and Khandaker (2010) performed seismic vulnerability assessment using AHP and GIS where different themes such as: building floors, building types, building age, resident population, population density, landuse/landcover etc were used to evaluate vulnerability against earthquakes. The steps generally followed in the vulnerability assessment are the identification of high risk areas by convolving Seismic Hazard Microzonation with vulnerability exposures in the GIS environment using AHP (Reveshty and

NHESSD
2, 3015–3063, 2014

Gharakhlou, 2009; Aghataher et al., 2008; Qunlin et al., 2013; Lantada et al., 2003 and Sarris et al., 2010). The AHP method avails to investigate the consistency of judgments to determine the significance of relative weight of factors (Reveshty and Gharakhlou, 2009). To determine the degree of consistency in judgments a consistency ratio is also measured from the AHP matrix. In the present investigation AHP has been applied to estimate the weights of different factors of vulnerability exposures for calculating the Risk Index (RI) in an attempt to generate multicriteria risk evolution protocol in both the socio-economic and structural implications. A combination of spatial/non-spatial exposures against earthquakes, the degree of vulnerability of each building element in terms of its typology, height and age, as also the socio-economic exposures have been measured. The associated features are ranked or scored within the theme. The initial integral ranking, X_j, is normalized to ensure that no layer exerts an influence beyond its determined weight using the following relation (Nath, 2004),

$$X_j = \frac{R_j - R_{\min}}{R_{\max} - R_{\min}} \tag{5}$$

Where, R_j are the row score, $R_{\max}$ and $R_{\min}$ are the maximum and minimum scores of a particular layer.

The socio-economic risk elements i.e. Population Density (PD) and Landuse/Landcover (LULC) are integrated over the Seismic Hazard Microzonation theme to demarcate the most vulnerable zones in view of socio-economic activities of the region. The Socio-Economic Risk Index (SERI) is calculated as,

$$\mathrm{SERI} = [\mathrm{SHM}_w \mathrm{SHM}_r + \mathrm{PD}_w \mathrm{PD}_r + \mathrm{LULC}_w \mathrm{LULC}_r] / \sum w \tag{6}$$

The ranks and weights for socio-economic vulnerability exposures over Seismic Hazard Microzonation are illustrated in Table 6. The concept of social vulnerability helps to identify those characteristics and experiences of individuals and communities that enable them to respond and to recover from earthquake hazards. The socio-economic seismic risk map of Kolkata is depicted in Fig. 14. Four broad divisions of socio-economic risk index (SERI) have been identified with Risk Index (SERI) defined as $0.75 < \text{SERI} \leq 1.0$ indicating severe risk condition in Salt Lake and patches of Central Kolkata area, $0.50 < \text{SERI} \leq 0.75$ indicating High seismic risk in most of the Central and North Kolkata, $0.25 < \text{SERI} \leq 0.50$ moderate risk in the most part of South, North-East and West Kolkata, while $\text{SERI} < 0.25$ presents a completely risk free regime.

The structural risk elements namely Building Typology (BT), Building Height (BH) and Building Age/growth (BA) have been integrated over the SHM depending on their contribution towards seismic vulnerability. The Structural Risk Index (SRI) due to the Structural Risk Exposures over the SHM are estimated as,

$$\text{SRI} = [\text{SHM}_w\text{SHM}_r + \text{BT}_w\text{BT}_r + \text{BH}_w\text{BH}_r + \text{BA}_w\text{BA}_r]/\sum w \quad (7)$$

The ranks and weights for structural vulnerability exposures over Seismic Hazard Microzonation are illustrated in Table 7. To determine the most and least structural vulnerable areas, the SRI scores are mapped as < 0.25 (low vulnerability) to ~ 1 (high vulnerability) as shown in Fig. 15. Four broad divisions have been identified with Structural Risk Index (SRI) defined as $0.75 < \text{SRI} \leq 1.0$ indicating severe risk condition in Salt Lake area, $0.50 < \text{SRI} \leq 0.75$ indicating High risk mostly in Central Kolkata, $0.25 < \text{SRI} \leq 0.50$ moderate risk in the most part of West Kolkata, while $\text{SRI} < 0.25$ presents a completely risk free regime. From the depiction of Fig. 15, it is easier to identify the most vulnerable buildings and therefore, the suggestion of their preventive measures. In Kolkata, most of the structural vulnerability index range from 0 to 0.50 indicating a lower vulnerability level. Detailed analyses and ground-truthing reveal that most of the buildings in the city are 1–4 storied where the resonance frequency of the soil column is between 1.0–2.0 Hz. On the other hand, an index > 0.5 is of higher vulnerability level in terms of both height and severity of structural damage being constructed on swamps and artificially non-engineered fills. In Central Kolkata most of the buildings exhibit high structural vulnerability because of its age (80 % $>$ 50 years) and unplanned construction. The damage distribution due to the Great 1934 Bihar Nepal

Earthquake of M_w 8.1 is identified in the severe to High Risk zones (marked by a star (*)). The detailed seismic vulnerability attributions are presented in Table 8.

In the present study, we have also calculated the design horizontal seismic coefficient (A_h) for the existing structures by the following expression;

$$A_h = Z_F I S_a / 2Rg \tag{8}$$

Where, Z_F = zone factor (taken from Nath et al., 2014), I = importance factor, depending upon the functional use of the structures, R = response reduction factor, depending on the perceived seismic damage performance of the structure and S_a/g = average response acceleration coefficient for rock or soil sites (Nath et al., 2014). BIS (2002) specified the values of "I" and "R" for all kinds of buildings. The sample seismic coefficient (A_h) distribution to be used for Kolkata for all kinds of structures with the predominant period of 1.0 s is depicted in Fig. 16. Depending upon the value of seismic coefficient (A_h) the category of building has been defined by BIS (2002) as given in Table 9. From Fig. 16 it is evident that the City may be suitable for "A" and "B" type of structures only. However "C" type of structures may also be built in the northeast part of the City.

The probability of damage in each seismic risk zone is calculated in relationship with the given ground motion parameters to evaluate the building performance for a particular seismic event. Based on RVS technique, we have selected four model type buildings viz. RM2L, RM2M, URML and URMM based on capacity curves given in NIBS (2002). In the present context, "RM2L", "RM2M" types represent "C" type structure while URML and URMM represent "B" type structure. We calculated the demand spectrum curve of spectral acceleration, the peak building response and the cumulative damage probabilities of all the four-model type buildings. The demand spectrum curve of spectral acceleration is a function of spectral displacement, spectral response at the period 0.3 and 1.0 s that has been used for the characterization of the ground motion demand. The spectral displacement has been determined by using the following equation;

$$S_D = 9.8 \cdot S_A \cdot T^2 \tag{9}$$

where, "S_A" = amplified spectral acceleration in "g" (Nath et al., 2014), "T" = time period (s) and "S_D" = spectral displacement (inches). The capacity curve represents the characteristics of a structure, which is a plot of lateral resistance of a building as a function of the characteristic lateral displacement. The capacity curve is characterized by three control points: design capacity, yield capacity, and ultimate capacity. The capacity curve parameters for four building types have been adopted from NIBS (2002). The peak building response is estimated from the interaction of the building capacity curve and the demand curve at the specified building location. The peak building response at the point of interaction of the capacity curve and the demand curve are used with fragility curve to estimate the damage state probability. Table 10 enlists the calculated peak building response values for all the four-model building types. The cumulative damage probabilities have been calculated as (NIBS, 2002),

$$p[d_s|S_d] = \Phi\left[\frac{1}{\beta_{d_s}} \ln\left(\frac{S_d}{\overline{S}_{d,d_s}}\right)\right] \quad (10)$$

Where, $p[d_s|S_d]$ = probability of being in or exceeding a damage state d_s; S_d = given spectral displacement (inches); $\overline{S}_{d_s}$ = median value of S_d at which the building reaches threshold of damage state d_s; β_{d_s} = lognormal standard deviation of spectral displacement of damage state, d_s; and Φ = standard normal cumulative distribution function. Table 11 enlists the cumulative damage probabilities of all four-model building types in terms of slight, moderate, extensive and complete hazard.

6 Conclusion

Seismic vulnerability and risk has emerged as an important issue in high risk urban centers across the globe and is considered an integral part of earthquake induced disaster mitigation practices. The adopted seismic risk framework is a multidimensional

NHESSD
2, 3015–3063, 2014

concept based on seismic hazard which include seismological, geological, geotechnical and geophysical database and the vulnerability exposures viz. population density, landuse/landcover, building typology, building height and building age judiciously integrated on Geographical Information System to identify those characteristics of buildings/socio-economic conditions which are responsible for earthquake disaster.

In Kolkata about 40 % buildings fall under the high risk zone in and around the central part of the city which is the oldest part of the Metropolitan whereas about 5–7 % buildings are in the severe risk zone, most of which are located in the artificial non engineered filled-up regions. Both the socio-economic and structural risk maps will contribute towards mitigation efforts against earthquake disaster of the City of Kolkata.

Acknowledgements. This work has been supported by the Ministry of Earth Sciences, Government of India vide sanction order no. MOES/P.O.(seismo)/1(60)/2009. Department of Disaster Management, Government of West Bengal facilitated smooth execution of the project.

References

Aghataher, R., Delavar, M. R., Nami, M. H., and Samnay, N.: A Fuzzy-AHP Decision Support System for Evaluation of Cities Vulnerability against Earthquakes, World Applied Sciences, IDOSI Publications, 3, 66–72, 2008.

BIS: IS 1893–2002 (Part 1): Indian Standard Criteria for Earthquake Resistant Design of Structures, Part 1 – General Provisions and Buildings, Bureau of Indian Standards, New Delhi, 2002.

BMTPC: Vulnerability Atlas of India: Earthquake, Windstorm and Flood Hazard Maps and Damaged Risk to Housing, Ministry of Housing & Urban poverty Alleviation, Government of India, First Revision, 1997.

Congalton, G. R.: Review of assessing the accuracy of classifications of remotely sensed data, Remote Sens. Environ., 37, 35–46, 1991.

Congalton, G. R. and Mead, R.: A quantitative method to test for consistency and correctness of photo interpretation, Photogramm. Eng. Rem. S., 49, 69–74, 1983.

Congalton, R. G. and Green, K.: Assessing the Accuracy of Remotely Sensed Data: Principles and Practices, CRC Press, Inc, Boca Raton, Florida, 137 pp., 1999.

Dasgupta, S., Sural, B., Harendranath, L., Mazumadar, K., Sanyal, S., Roy, A., Das, L. K., Misra, P. S., and Gupta, H.: Seismotectonic Atlas of India and its Environs, Geological Survey of India, Calcutta, India, 2000.
Geneletti, D. and Gortea, H. G. B.: A method for object-oriented land cover classification combining Landsat TM data and aerial photographs, Int. J. Remote Sens., 24, 1237–1286, 2003.
GSI: The Bihar-Nepal Earthquake of 1934, Geol. Surv. India Mem., 73, 391 pp., 1939.
Idriss, I. M. and Boulanger, R. W.: Semi-empirical procedures for evaluating liquefaction potential during earthquakes, Soil Dyn. Earthq. Eng., 26, 115–130, 2006.
Ishita, R. P. and Khandaker, S.: Application of analytical hierarchical process and GIS in earthquake vulnerability assessment: case study of Ward 37 and 69 in Dhaka City, Journal of Bangladesh Institute of Planners, 3, 103–112, 2010.
Iwasaki, T., Tokida, K., Tatsuoka, F., Watanabe, S., Yasuda, S., and Sato, H.: Microzonation for soil liquefaction potential using simplified methods, in: Proceedings of the 3rd International Conference on Microzonation, Seattle, 3, 1319–1330, 1982.
Jensen, J. R.: Introductory Digital Image Processing: a Remote Sensing Perspective, 2nd. edn., Prentice Hall Inc., Upper Saddle River, New Jersey, USA, 1996.
Kramer, S. L.: Geotechnical Earthquake Engineering, Prentice Hall, Upper Saddle River, NJ, 653 pp., 1996.
Kundu, A. K. and Aag, P.: Atlas of the City of Calcutta & its Environs, National Atlas and Thematic Mapping Organization, Ministry of Science and Technology, Government of India, 1996.
Lantada, N., Pujades, L. G., and Barbat, A.: Vulnerability and seismic damage scenarios for Barcelona (Spain) by using GIS, Geophys. Res. Abstr., 5, 09103, available at: http://adsabs.harvard.edu/abs/2003EAEJ, 2003.
Landis, J. R. and Koch, G. G.: The measurement of observer agreement for categorical data, Biometrics, 33, 159–174, 1977.
Lermo, J. and Chilvez-Garcfa, F. J.: Site effect evaluation using spectral ratios with only one station, B. Seismol. Soc. Am., 83, 1574–1594, 1993.
Lu, D. and Weng, Q.: Urban classification using full spectral information of Landsat ETM Imagery in Marion County, Indiana, Photogramm. Eng. Rem. S., 71, 1275–1284, 2005.
McGuire, R. K.: Seismic Hazard and Risk Analysis, EERI Publication, No MN0-10, 2004.
Middlemiss, C. S.: Two Calcutta Earthquakes of 1906, Records Geol. Surv. Ind., 36, 214–232, 1908.

Nakamura, Y.: A method for dynamic characteristics estimations of subsurface using microtremors on the ground surface, QR RTRI, 30, 25–33, 1989.
Nath, S. K.: Seismic hazard mapping in sikkim himalaya through GIS integration of site effects and strong ground motion attributes, Nat. Hazards, 31, 319–342, 2004.
Nath, S. K. and Thingbaijam, K. K. S.: Seismic hazard assessment – a holistic microzonation approach, Nat. Hazards Earth Syst. Sci., 9, 1445–1459, doi:10.5194/nhess-9-1445-2009, 2009.
Nath, S. K., Thingbaijam, K. K. S., Vyas, J. C., Sengupta, P., and Dev, S. M. S. P.: Macroseismic-driven site effects in the southern territory of West Bengal, India, Seismol. Res. Lett., 81, 480–487, 2010.
Nath, S. K., Adhikari, M. D., Maiti, S. K., Devaraj, N., Srivastava, N., and Mohapatra, L. D.: Earthquake scenario in West Bengal with emphasis on Seismic Hazard Microzonation of the city of Kolkata, India, Nat. Hazards Earth Syst. Sci., under review, 2014.
NIBS: HAZUS99 – earthquake loss estimation methodology, technical manual, in: Technical Manual, edited by: FEMA, Federal Emergency Management Agency (FEMA), National Institute of Building Sciences (NIBS), Washington DC, 325 pp., 2002.
O'Malley, J.: US Geological Survey ArcMap Sediment Classification Tool: Installation and User Guide, USGS, Open-File Report 2007-1186, 2007
Panahi, M., Rezaie, F., and Meshkani, S. A.: Seismic vulnerability assessment of school buildings in Tehran city based on AHP and GIS, Nat. Hazards Earth Syst. Sci. Discuss., 1, 4511–4538, doi:10.5194/nhessd-1-4511-2013, 2013.
Qunlin, J., Bai, P., and Duan, Q.: Risk assessment on Beijing urban infrastructure vulnerability, in: Proceedings of the 2nd International Conference on Systems Engineering and Modeling (ICSEM-13), Atlantis Press, Paris, France, 2013.
Reveshty, M. A. and Gharakhlou, M.: Modeling of Urban Building Vulnerability in Earthquake against using Analytical Hierarchy Process (AHP) and GIS, a Case Study on Zanjan City, Northwest of Iran, available at: http://www.mapasia.org/2009/proceeding/urban_regional/ma09Mohsen.pdf, 2009.
Roy, P. K., Banerjee, G., Mazumdar, A., Kar, A., Majumder, A., and Roy, M. B.: A study to ascertain the optimum yield from groundwater source in the eastern part of Kolkata municipal corporation area in West Bengal, India, European Journal of Sustainable Development, 1, 97–112, 2012.

NHESSD
2, 3015–3063, 2014

Seismic vulnerability and risk assessment of Kolkata City, India

S. K. Nath et al.

Saaty, T. L.: The Analytic Hierarchy Process, McGraw-Hill International, New York, NY, USA, 1980.
Sarris, A., Loupasakis, C., Soupios, P., Trigkas, V., and Vallianatos, F.: Earthquake vulnerability and seismic risk assessment of urban areas in high seismic regions: application to Chania City, Crete Island, Greece, Nat. Hazards, 54, 395–412, 2010.
Sinha, R. and Adarsh, N.: A postulated earthquake damage scenario for Mumbai, ISET Journal of Earthquake Technology, 36, 169–183, 1999.
Small, C.: Multi-temporal analysis of urban reflectance, Remote Sens. Environ., 81, 427–442, 2002.
Story, M. and Congalton, G. R.: Accuracy assessment: a user's perspective, Photogramm. Eng. Rem. S., 52, 397–399, 1986.
Youd, T. L., Idriss, I. M., Andrus, R. D., Arango, I., Castro, G., Christian, J. T., Dobry, R., Finn, W. D. L., Harder Jr, L. F., Hynes, M. E., Ishihara, K., Koester, J. P., Liao, S. S. C., Marcuson-III, W. F., Martin, G. R., Mitchell, J. K., Moriwaki, Y., Power, M. S., Robertson, P. K., Seed, R. B., and Stokoe II, K. H.: Liquefaction resistance of soils: summary report from the 1996 NCEER and 1998 NCEER/NSF workshops on evaluation of liquefaction resistance of soils, J. Geotech. Geoenviron., 127, 817–833, 2001.
Zha, Y., Gao, J., and Ni, S.: Use of normalized difference built-up index in automatically mapping urban areas from TM imagery, Int. J. Remote Sens., 24, 583–594, 2003.
Zhang, Q., Wang, J., Peng, X., Gong, P., and Shi, P.: Urban built-up land change detection with road density and spectral information from multi-temporal Landsat TM data, Int. J. Remote Sens., 23, 3057–3078, 2002.

Table 1. Population growth of urban Kolkata during 1901–2011 (Census, 2011; http://censusindia.gov.in/).

No	Years	Population	Variation	% Increase
1.	1901	1 510 008	–	–
2.	1911	1 745 198	235 190	15.58
3.	1921	1 884 584	139 386	7.99
4.	1931	2 138 563	253 979	13.48
5.	1941	3 621 413	1 482 850	69.34
6.	1951	4 669 559	1 048 146	28.94
7.	1961	5 983 669	1 314 110	28.14
8.	1971	7 420 300	1 436 631	24.01
9.	1981	9 194 018	1 773 718	23.90
10	1991	11 021 918	1 827 900	19.88
11.	2001	13 205 697	2 183 779	19.81
12.	2011	14 112 536	906 839	7.6

NHESSD
2, 3015–3063, 2014

Table 2. Error matrix derived for landuse/landcover mapping in Kolkata.

Satellite Image (LISS-IV) based LULC (classified data)	GPS based ground truth (reference data)										User's accuracy
	RCIA	RPWC	PL	OS	VG	SL	DFL	AL	CL	Total	
RCIA	452	0	0	5	0	0	0	10	0	467	96.78
RPWC	0	43	0	0	0	15	0	0	0	58	74.13
PL	0	0	37	0	11	0	0	2	5	55	67.27
OS	12	0	0	32	0	3	11	3	1	62	51.61
VG	0	0	17	0	89	2	5	7	3	123	72.35
SL	0	7	0	0	3	98	11	5	3	127	77.16
DFL	0	0	0	5	0	0	37	9	3	54	68.51
AL	17	0	0	3	5	7	13	71	18	134	52.98
CL	0	0	2	1	9	3	5	11	85	116	73.27
Total	581	50	56	46	117	128	82	118	118		
Producer's Accuracy	93.97	86.00	66.1	78.0	76.0	76.6	45.1	65.7	72.0		
Overall Accuracy										78.92	
Normalized Accuracy										70.00	
Kappa value										0.733	
Kappa Variance										0.0002	

Residential commercial and industrial area (RCIA), river/pond/waterbody/canal (RPWC), plantation (PL), open space (OS), vegetation (VG), swampy land (SL), dry fellow land (DFL), arable land (AL), cultivated land (CL).

Table 3. Error matrix derived for building typology in Kolkata.

		Rapid Visual Screening based building typology (reference data)						User's accuracy
		A1	A2	B	C1-i	C1-ii	Total	
Satellite Image based building typology (classified data)	A1	105	29	19	11	7	171	61.4
	A2	27	128	25	15	11	206	62.1
	B	11	19	93	13	6	142	65.5
	C1-i	12	17	26	243	37	335	72.5
	C1-ii	5	9	13	42	271	340	79.7
	Total	160	202	176	324	332		
	Producer's Accuracy	65.6	63.3	52.8	75.0	81.6		
			Overall Accuracy					70.4
			Normalized Accuracy					68.1
			Kappa value					0.61
			Kappa Variance					0.00028

A1 – Mud and unburnt brick wall; A2 – stone wall; B – burnt brick wall; C1-i: concrete wall; C1-ii: newly built-up concrete building.

NHESSD
2, 3015–3063, 2014

Table 4. Error matrix derived for building growth/age during 2005–2010 in Newtown, Kolkata.

Urban growth using multi-temporal Landsat TM data (classified data)	Urban Expansion based on Google Earth Imageries (reference data)				User's accuracy
		High Expansion	Low Expansion	Total	
	High Expansion	678	69	747	90.7
	Low Expansion	93	281	374	75.1
	Total	771	350		
	Producer's Accuracy	87.9	80.3		
		Overall Accuracy			85.5
		Normalized Accuracy			84.4
		Kappa value			0.67
		Kappa Variance			0.00056

NHESSD
2, 3015–3063, 2014

Table 5. Error matrix derived for building height in Kolkata.

Google Earth 3-D aspect based building height (classified data)	Houses (1 F)	Buildings (2–4 F)	Tall (5–8 F)	Multistoried (9–10 F)	Skyscrapers (> 10 F)	Total	User's accuracy
	Rapid Visual Screening based building height (reference data)						
Houses (1 F)	247	49	0	0	0	296	83.4
Buildings (2–4 F)	55	298	27	0	0	380	78.4
Tall Buildings (5–8 F)	0	29	195	19	0	243	80.2
Multistoried Buildings (9–10 F)	0	0	10	128	24	162	79.0
Skyscrapers (> 10 F)	0	0	0	18	97	115	84.3
Total	302	376	232	165	121		
Producer's Accuracy	81.8	79.3	84.1	77.6	80.2		
Overall Accuracy							80.6
Normalized Accuracy							80.5
Kappa value							0.74
Kappa Variance							0.00022

NHESSD
2, 3015–3063, 2014

Table 6. Normalized weights and ranks assigned to respective themes and the features of socio-economic risk attributes for thematic integration on GIS.

Themes	Weight	Attributes	Rating	Normalized Rating
Seismic Hazard Microzonation and socio-economic seismic vulnerability exposures				
Seismic Hazard Microzonation (SHM)	0.50	Low	1	0.0000
		Moderate	2	0.3333
		High	3	0.6666
		Severe	4	1.0000
Population density (km^2)	0.33	< 1000	1	0.0000
		1001–3000	2	0.1111
		3001–5000	3	0.2222
		5001–15 000	4	0.3333
		15 001–30 000	5	0.4444
		30 001–50 000	6	0.5556
		50 001–70 000	7	0.6667
		70 001–90 000	8	0.7778
		90 001–110 000	9	0.8889
		> 110 000	10	1.0000
Landuse/landcover	0.17	Water body, Pond, River, Canal	1	0.0000
		Open Space	2	0.1250
		Swampy Land	3	0.2500
		Dry Fellow Land	4	0.3750
		Vegetation/grassland	5	0.5000
		Plantation	6	0.6250
		Arable Land	7	0.7500
		Cultivated Land	8	0.8750
		Residential, commercial and industrial area	9	1.0000

NHESSD
2, 3015–3063, 2014

NHESSD
2, 3015–3063, 2014

Table 7. Normalized weights and ranks assigned to respective themes and the features of structural risk attributes for thematic integration on GIS.

Themes	Weight	Attributes	Rating	Normalized Rating
Seismic Hazard Microzonation and structural seismic vulnerability exposures				
Seismic Hazard Microzonation (SHM)	0.40	Low	1	0.0000
		Moderate	2	0.3333
		High	3	0.6666
		Severe	4	1.0000
Building typology	0.30	A1 – mud and urban brick wall	1	0.0000
		A2 – stone wall	2	0.3333
		B – burnt bricks building	3	0.6666
		C1-i concrete building and C1-ii newly built concrete building	4	1.0000
Building height	0.20	Houses (1 F)	1	0.0000
		Buildings (2–4 F)	2	0.2500
		Tall Buildings (5–8 F)	3	0.5000
		Multistoried Buildings (9–10 F)	4	0.7500
		Skyscrapers (> 10 F)	5	1.0000
Building age in years	0.10	New building	1	0.0000
		10	2	0.1667
		20	3	0.3333
		30	4	0.5000
		35	5	0.6667
		40	6	0.8333
		> 50	7	1.0000

Table 8. Structural Risk Level with corresponding vulnerability exposures at selective locations in Kolkata.

Sl.	Lat (° N)	Long (° E)	LM	SRI	P_F	LPI	I_{MMI}	PD	BH	BA	BT
1	22.4940	88.311	Behala	High	1.4	3.3	VI	34 814	Houses (1 F)	10	B – Burnt Bricks Building
2	22.5125	88.388	Rajdanga	Moderate	1.5	12.1	VI	13 935	Houses (1 F)	30	C1-i Concrete Building
3	22.5971	88.367	Shyambazar	High	2.4	13.5	VI	76 950	Buildings (2–4 F)	40	C1-i Concrete Building
4	22.6346	88.424	Dum Dum	High	1.4	4.7	VII	12 208	Buildings (2–4 F)	40	C1-i Concrete Building
5	22.6468	88.344	Bali	Moderate	1.5	4.9	VI	19 025	Buildings (2–4 F)	5	B – Burnt Bricks Building
6	22.6190	88.305	Kona	Moderate	1.4	9.4	VI	9453	Buildings (2–4 F)	35	C1-i Concrete Building
7	22.5037	88.252	Maheshtala	Low	1.4	3.6	VI	7401	Houses (1 F)	40	C1-i Concrete Building
8	22.5269	88.327	Alipur	High	1.7	10.1	VI	11 225	Tall Buildings (5–8 F)	10	C1-i Concrete Building
9	22.5470	88.287	Metiaburuz	High	1.4	4.6	VI	158 703	Tall Buildings (5–8 F)	30	C1-i Concrete Building
10	22.4556	88.422	Dabpur	Moderate	1.7	27.5	VI	6283	Buildings (2–4 F)	30	B – Burnt Bricks Building
11	22.4938	88.379	Jadabpur	High	1.5	13.5	VI	26 343	Tall Buildings (5–8 F)	40	C1-i Concrete Building
12	22.5182	88.342	Kalighat	Moderate	1.4	4.2	VI	51 318	Buildings (2–4 F)	50	A2 – Stone Wall
13	22.4906	88.451	Deora	Low	1.4	21.2	VI	2528	Buildings (2–4 F)	5	B – Burnt Bricks Building
14	22.5092	88.379	Dhakuria	High	0.9	14.3	VI	21 802	Tall Buildings (5–8 F)	10	C1-ii Newly Builtup Concrete B
15	22.4604	88.317	Thakurpukur	Low	1.5	3.8	VI	13 477	Houses (1 F)	20	C1-i Concrete Building
16	22.5817	88.328	HAORA	High	1.3	14.0	VI	91 589	Houses (1 F)	50	C1-i Concrete Building
17	22.6283	88.347	Belur	High	2.0	11.8	VI	38 370	Houses (1 F)	50	B – Burnt Bricks Building
18	22.5151	88.457	Bakdoba	Moderate	1.4	12.7	VI	1234	Houses (1 F)	30	B – Burnt Bricks Building
19	22.6142	88.382	Paikpara	High	1.2	12.1	VI	41 056	Buildings (2–4 F)	50	C1-i Concrete Building
20	22.5527	88.354	Park Street	Severe	1.4	24.4	VI	8361	Multistoried Buildings (9–10 F)	25	C1-i Concrete Building
21	22.5830	88.416	Salt Lake	Severe	1.2	28.1	VII	13 075	Tall Buildings (5–8 F)	10	C1-ii Newly Builtup Concrete B
22	22.5854	88.480	New Town	Moderate	1.2	26.5	VII	1218	Buildings (2–4 F)	5	C1-ii Newly Builtup Concrete B
23	22.6030	88.468	Rajarhat	Moderate	0.9	34.3	VII	4195	Buildings (2–4 F)	5	C1-ii Newly Builtup Concrete B

P_F: predominant frequency; LPI: Liquefaction Potential Index; I_{MMI}: predicted MMI intensity; SRL: Structural Risk Level; LM: major land marks; PD: population density within the block; BH: building height; BA: building age (yr.); BT: building type as per BMTPC.

Table 9. Classification of building categories based on A_h (BIS, 2002).

Range of A_h	Building category	Description
< 0.05	A	Building in field-stone, rural structures, unburnt-brick houses, clay houses
0.05 to 0.06	B	Ordinary brick buildings, buildings of large block and prefabricated type, half timbered structures, buildings in natural hewn stone
0.06 to 0.08	C	Reinforced buildings, well built wooden structures
0.08 to 0.12	D	Other type not covered in
> 0.12	E	A, B, C

NHESSD
2, 3015–3063, 2014

NHESSD
2, 3015–3063, 2014

Table 10. Peak building response estimated for four significant model building types.

Model	Peak Building Response (Inches)			
Building	RM2L	RM2M	URML	URMM
Type	Reinforced Masonry Bearing Wall with Precast concrete diaphragms, Low rise (1–3 stories)	Reinforced Masonry Bearing Wall with Precast concrete diaphragms, Low rise (4–7 stories)	Unreinforced Masonry Bearing Wall, Low rise (1–2 stories)	Unreinforced Masonry Bearing Wall, Low rise (3+ stories)
S_D (inch)	0.71	0.727	0.639	0.735

Table 11. Estimated cumulative damage probabilities of four model building types defined in Table 10.

Model	Cumulative Probabilities			
Type	Slight	Moderate	Extensive	Complete
RM2L	0.4993	0.3113	0.0997	0.0041
RM2M	0.2843	0.1346	0.0060	0.0015
URML	0.6936	0.4312	0.1570	0.0350
URMM	0.5813	0.2640	0.0487	0.0065

NHESSD
2, 3015–3063, 2014

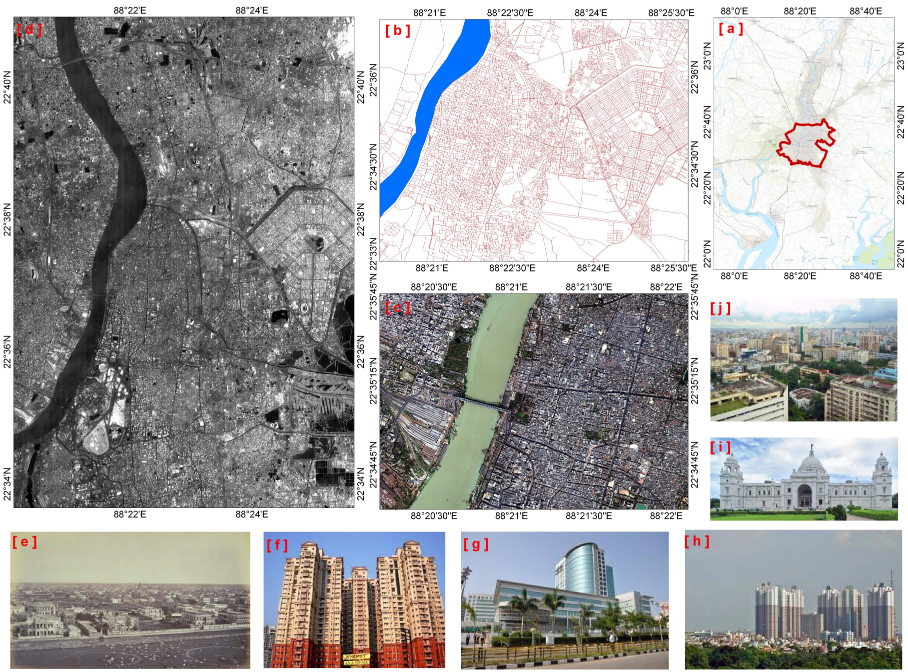

Fig. 1. Pilot Study area of Kolkata **(a)** Google Map showing the urban region of Kolkata, **(b)** road network of central part of the city, **(c)** GEO-eye (http://www.esri.com/data/basemaps) image of central Kolkata, **(d)** Cartosat-1 DEM represents the dense urban settlement of central Kolkata and Salt lake region, **(e–j)** representative old structure, skyscraper, steel structure, multi storied structures of the city.

NHESSD

2, 3015–3063, 2014

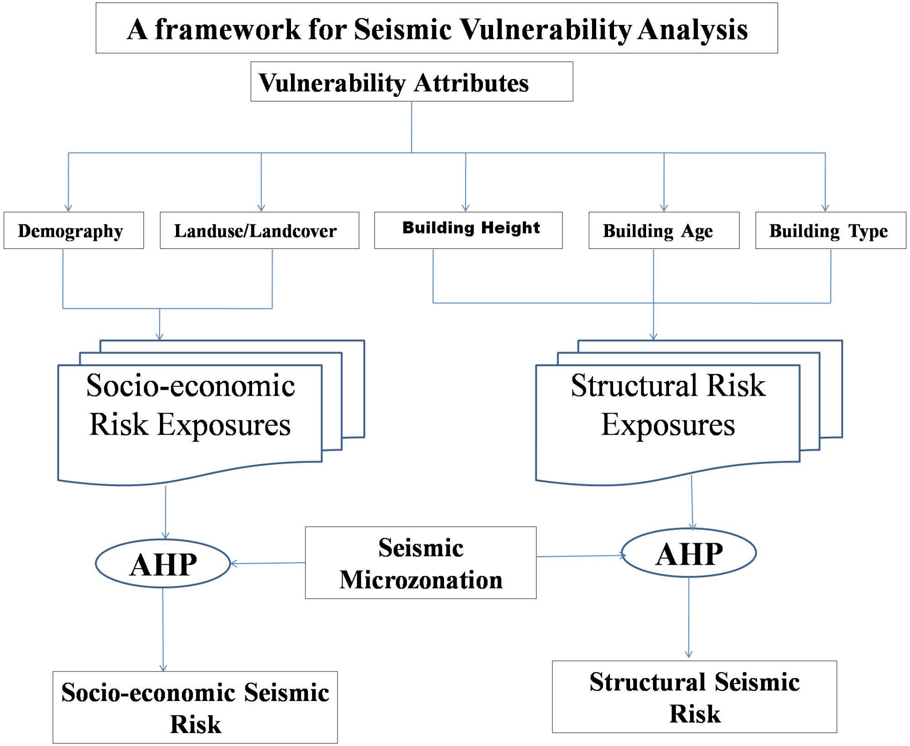

Fig. 2. Seismic vulnerability assessment protocol.

NHESSD
2, 3015–3063, 2014

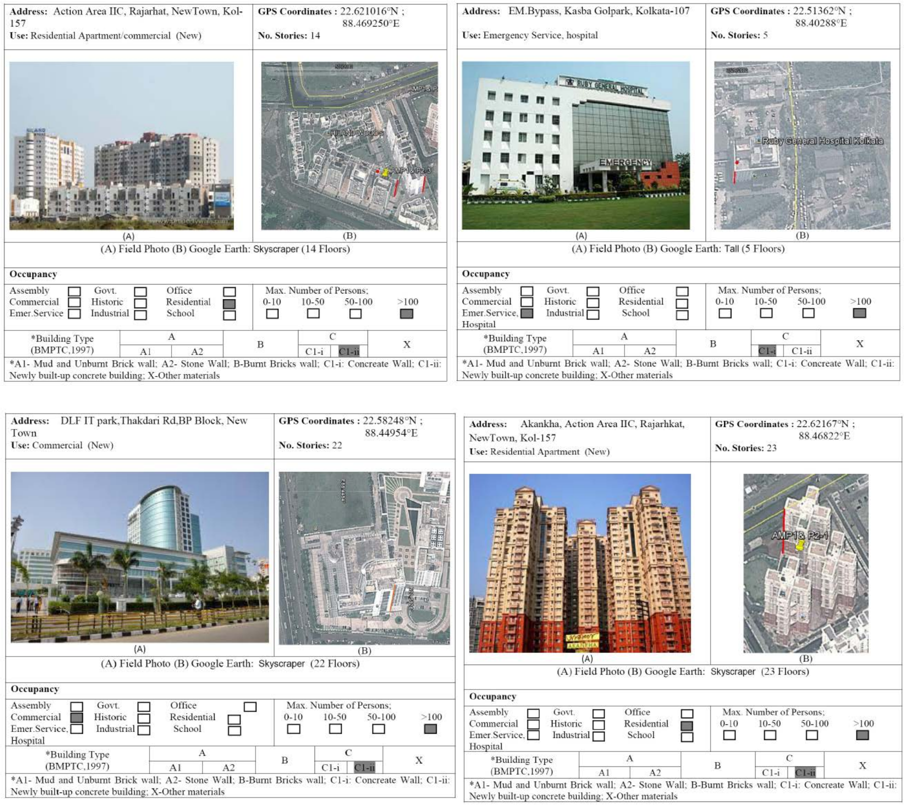

Fig. 3. Rapid Visual Screening (RVS) survey (at about 1200 sites) for field and Google Earth comparisons of existing building height in urban Kolkata for potential seismic vulnerability assessment.

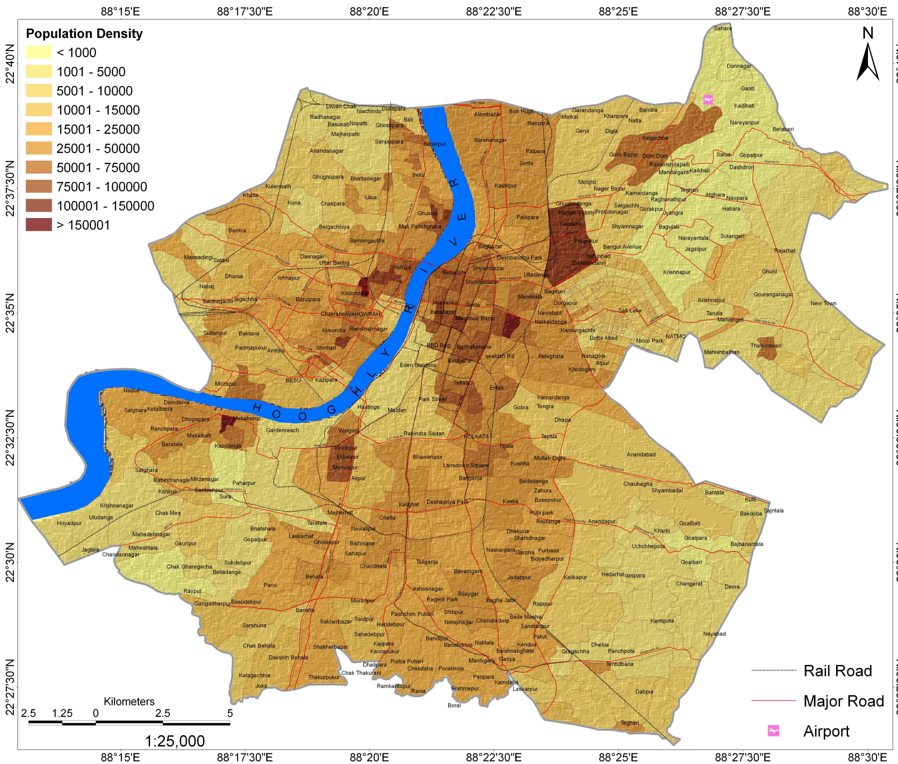

Fig. 4. Population density distribution of Kolkata after 2011 Census data.

NHESSD
2, 3015–3063, 2014

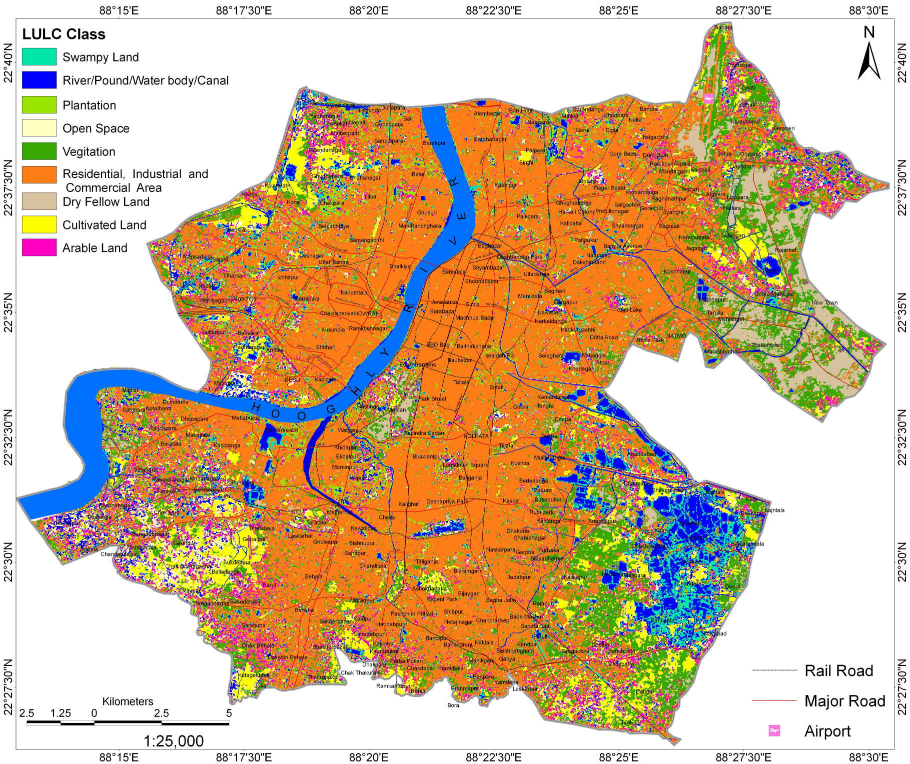

Fig. 5. Landuse/landcover map of Kolkata generated using LISS IV and PAN imagery.

NHESSD
2, 3015–3063, 2014

Seismic vulnerability and risk assessment of Kolkata City, India

S. K. Nath et al.

Fig. 6. Building typology distribution map of Kolkata derived using LISS IV and LANDSAT TM imagery.

NHESSD
2, 3015–3063, 2014

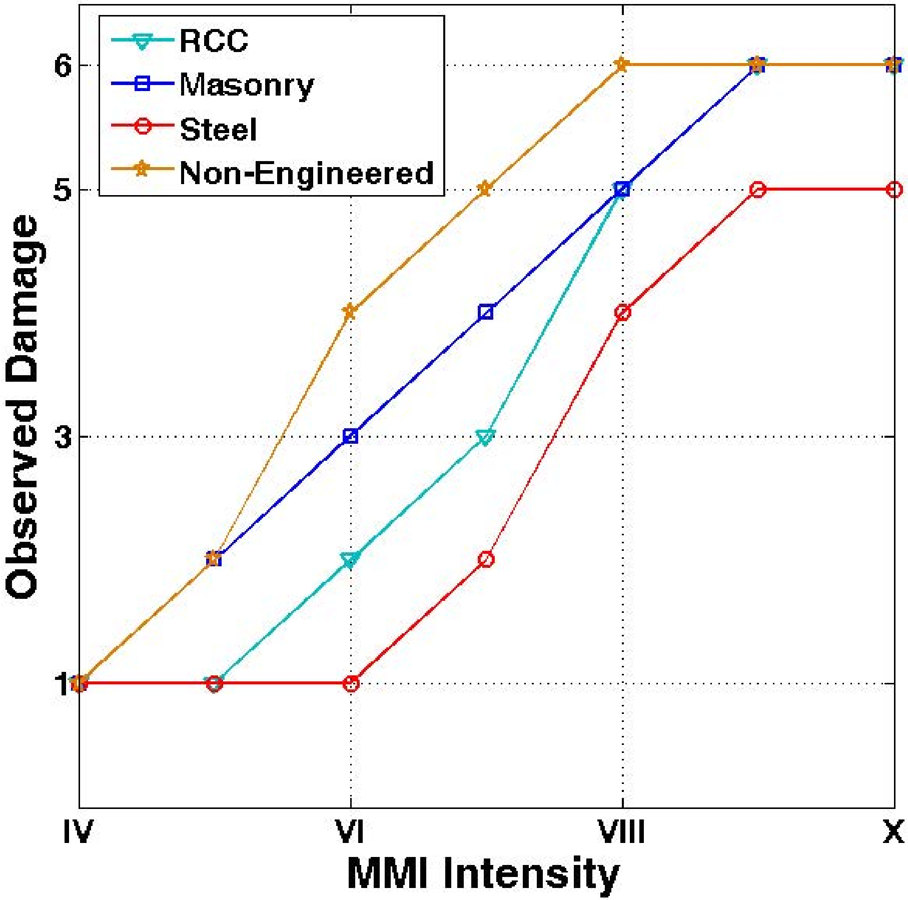

Fig. 7. Vulnerability curves for observed damage inflicted by the 1934 Bihar-Nepal Earthquake of M_w 8.1 (GSI, 1939) on various building typology in Kolkata and adjoining regions based on Sinha and Adarsh (1999).

NHESSD
2, 3015–3063, 2014

Seismic vulnerability and risk assessment of Kolkata City, India

S. K. Nath et al.

Title Page
Abstract | Introduction
Conclusions | References
Tables | Figures
◀| |▶
◀ ▶
Back | Close
Full Screen / Esc
Printer-friendly Version
Interactive Discussion

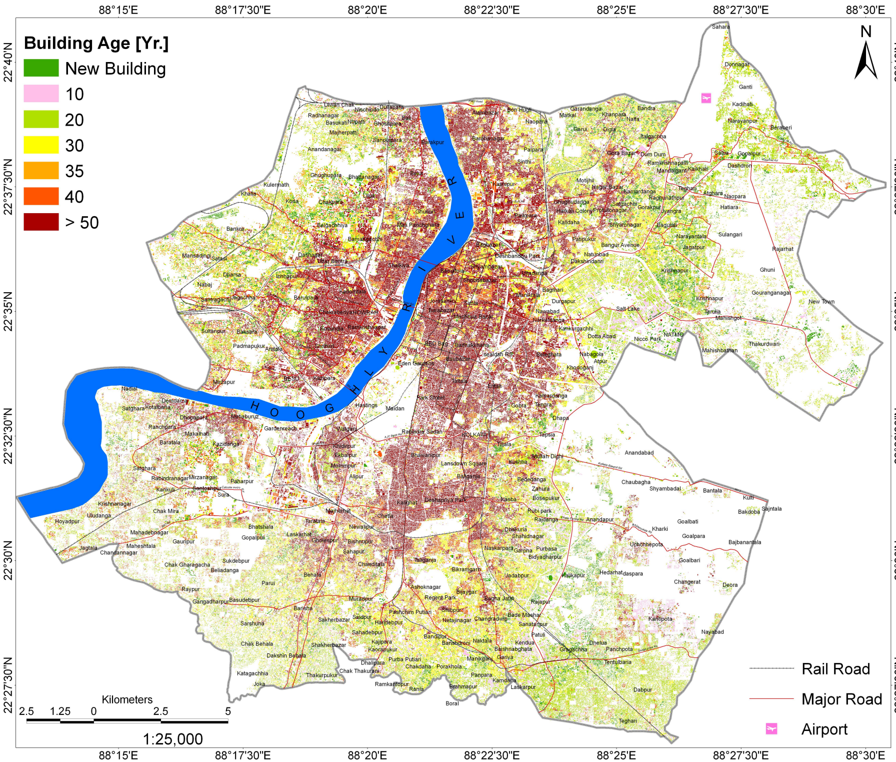

Fig. 8. Building age classification map of Kolkata using multi-temporal LANDSAT MSS, TM and ETM data for the period of 1975–2010.

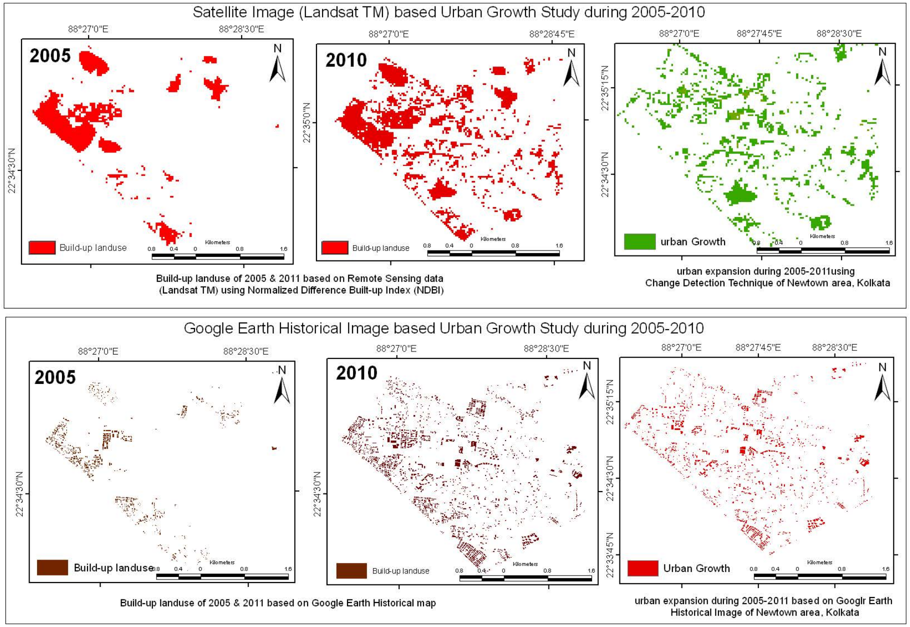

Fig. 9. Urban expansion during the period 2005–2010 based on both Landsat TM and Google Earth imageries.

NHESSD
2, 3015–3063, 2014

Seismic vulnerability and risk assessment of Kolkata City, India

S. K. Nath et al.

Fig. 10. Building height distribution map of Kolkata using Google Earth.

NHESSD

2, 3015–3063, 2014

Seismic vulnerability and risk assessment of Kolkata City, India

S. K. Nath et al.

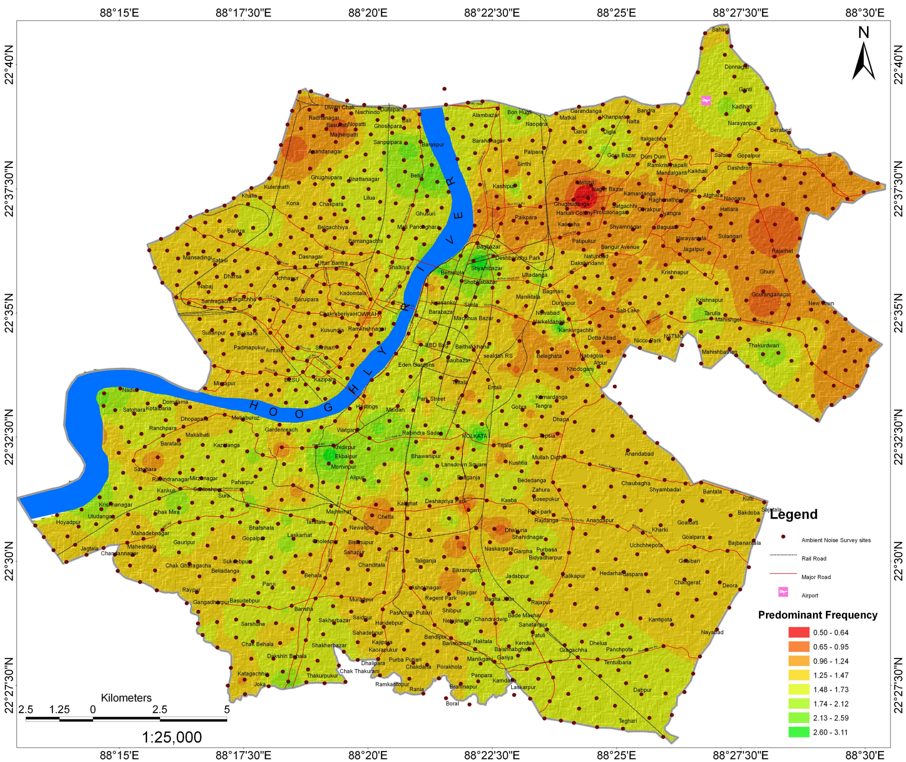

Fig. 11. Spatial distribution of predominant frequency in Kolkata as obtained from Ambient Noise Survey at 1200 locations and processing those by Nakamura ratio.

NHESSD
2, 3015–3063, 2014

Seismic vulnerability and risk assessment of Kolkata City, India

S. K. Nath et al.

Title Page
Abstract Introduction
Conclusions References
Tables Figures
◀| |▶
◀ ▶
Back Close
Full Screen / Esc
Printer-friendly Version
Interactive Discussion

NHESSD
2, 3015–3063, 2014

Seismic vulnerability and risk assessment of Kolkata City, India

S. K. Nath et al.

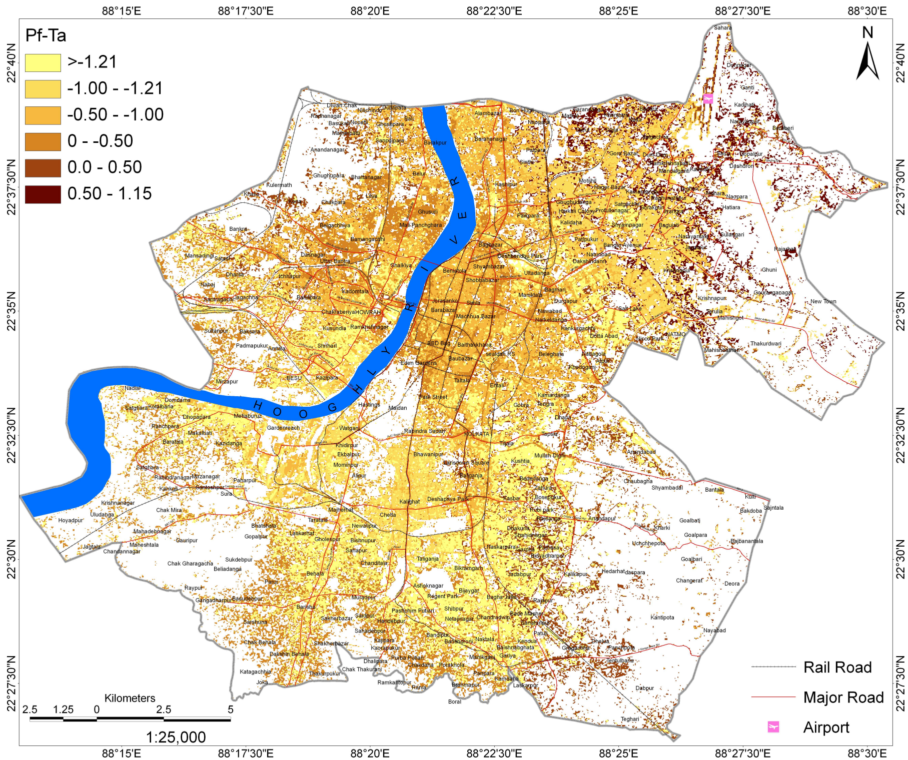

Fig. 12. The difference between the natural period of vibration of structure and the predominant period of the respective site indicating damage possibilities of existing structures/logistics.

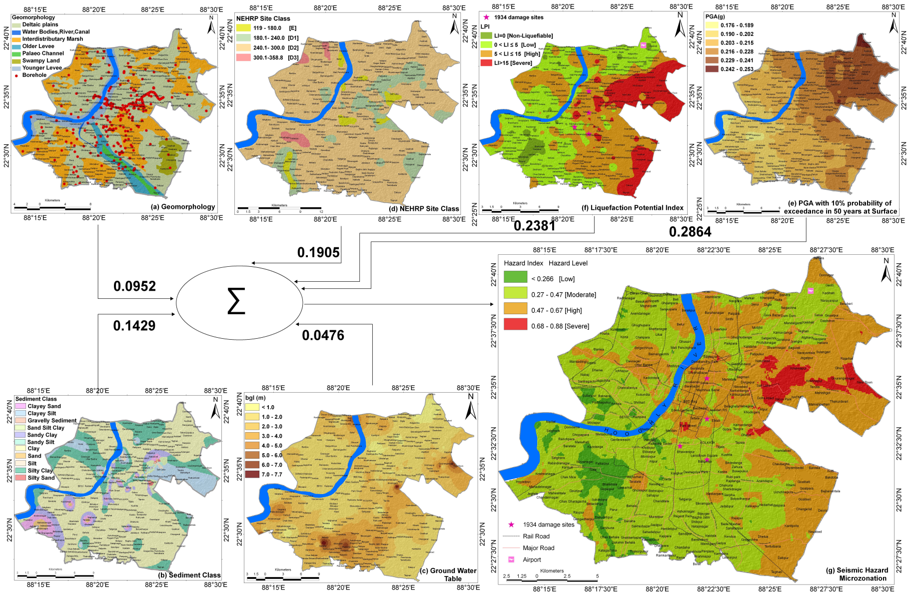

Fig. 13. Seismic Hazard Microzonation protocol for Kolkata showing the weights assigned to each theme labeled according to hazard contribution, **(a)** geomorphology **(b)** sediment class, **(c)** ground water table, **(d)** NEHRP site class, **(e)** spatial distribution of PGA in Kolkata with 10 % probability of exceedance in 50 years at Surface, **(f)** Liquefaction Potential Index (LPI) Distribution, and **(g)** Seismic Hazard Microzonation map of Kolkata.

NHESSD
2, 3015–3063, 2014

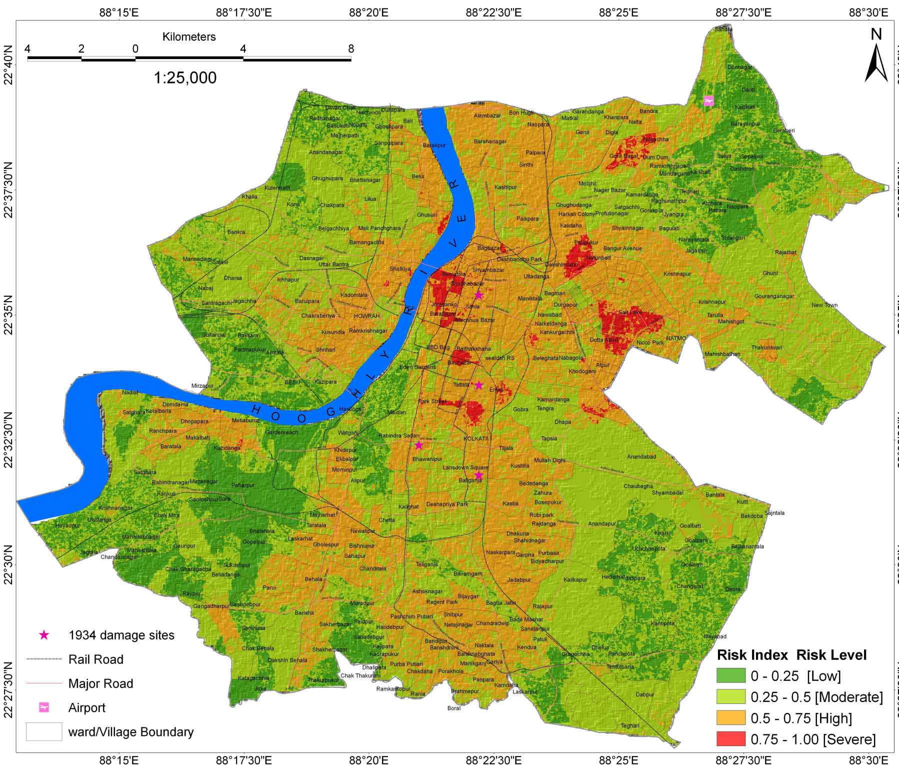

Fig. 14. Probabilistic seismic socio-economic risk map of Kolkata. Four broad divisions have been identified with Risk Index (SERI) defined as: $0.75 < \text{SERI} \leq 1.0$ indicating severe risk condition in Salt Lake area and a patch at central Kolkata, $0.50 < \text{SERI} \leq 0.75$ indicating High risk in central and north Kolkata, $0.25 < \text{SERI} \leq 0.50$ indicating moderate risk in the most part of southeast, northeast and west Kolkata, while $\text{SERI} < 0.25$ presents a completely risk free regime. The damage distribution due to the 1934 Bihar Nepal Earthquake of M_w 8.1 (GSI, 1939) are identified in the high risk zone (marked by a star (*)).

NHESSD
2, 3015–3063, 2014

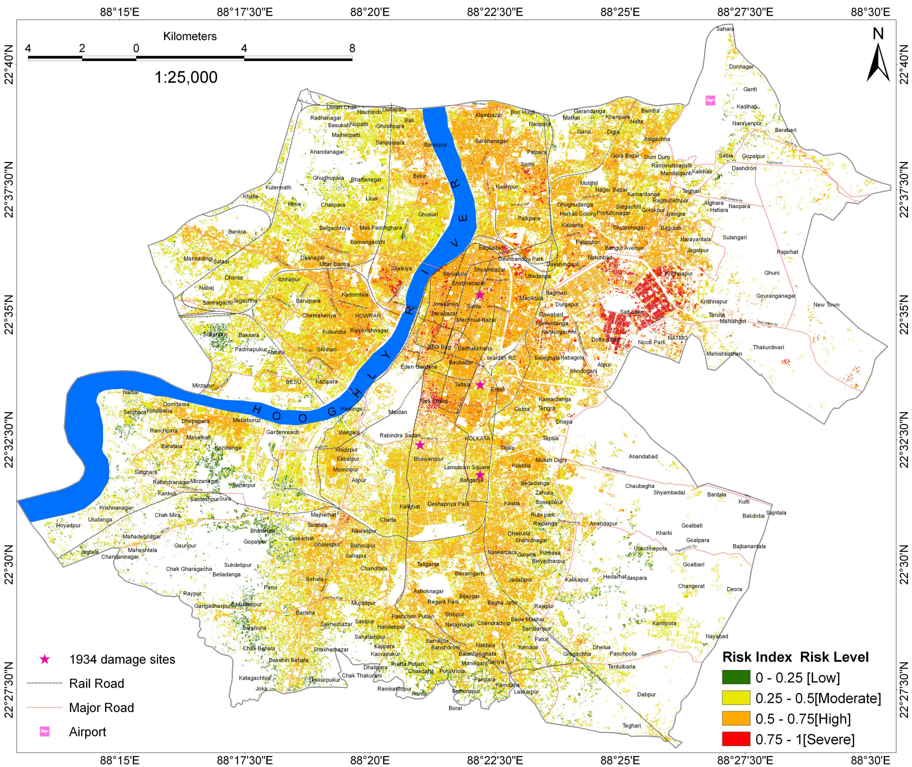

Fig. 15. Probabilistic seismic structural risk map of Kolkata. Four broad divisions have been identified with Risk Index (SRI) defined as: $0.75 < \text{SRI} \leq 1.0$ indicating severe risk condition in Salt Lake area, $0.50 < \text{SRI} \leq 0.75$ indicating high risk mostly in central Kolkata, $0.25 < \text{SRI} \leq 0.50$ depicting moderate risk in the most part of West Kolkata, while $\text{SRI} < 0.25$ presents a completely risk free regime. The damage distribution due to the 1934 Bihar Nepal Earthquake of M_w 8.1 (GSI, 1939) are identified in the high risk zone (marked by a star (*)). The detailed structural attributions are presented in Table 8.

NHESSD
2, 3015–3063, 2014

Title Page
Abstract | Introduction
Conclusions | References
Tables | Figures
◂◂ | ▸▸
◂ | ▸
Back | Close
Full Screen / Esc
Printer-friendly Version
Interactive Discussion

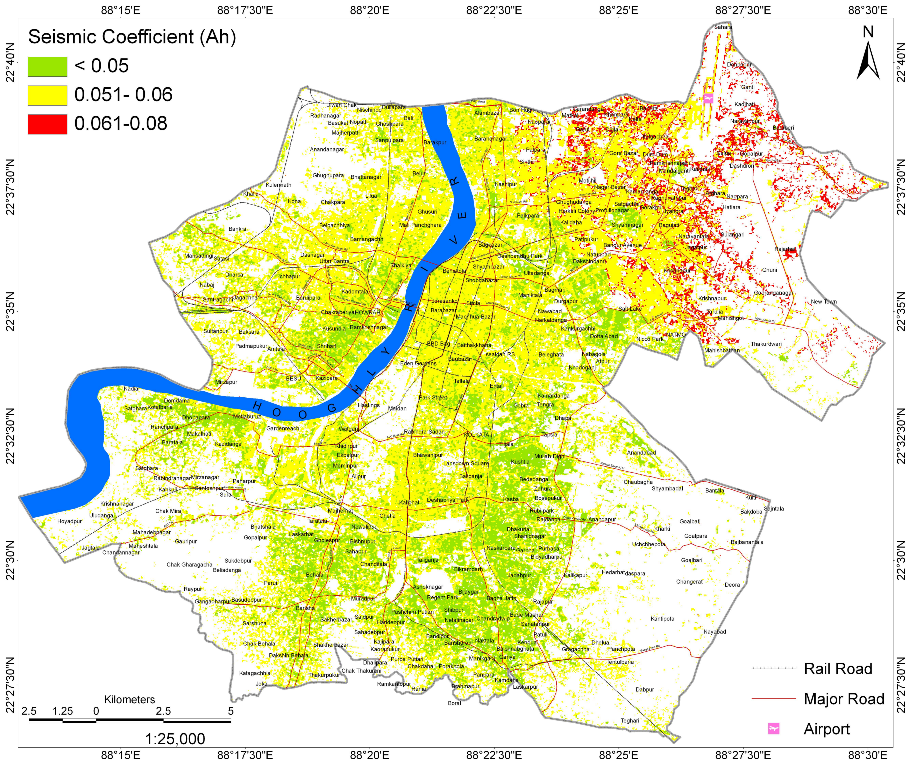

Fig. 16. Spatial distribution of horizontal seismic coefficient (A_h) to be used for Kolkata for structures with 1.0 s predominant period.